UNDERWATER LASER IMAGING

Shelby Metoyer, Darek Bogucki

Texas A&M University-Corpus Christi, Corpus Christi, Texas, United States

ABSTRACT

Attenuation of light in the ocean ranges widely depending on the environment and is especially significant in optical remote sensing. Absorption of light by ocean water limits the range light can travel before being extinguished. The complex interactions of scattering light and ocean water often lead to distortions of the signal as it propagates which degrades the quality and accuracy of underwater measurements. Consequently, underwater visibility (i.e. how well an object can be seen with definition at distance) can be less than 1 [m] in turbid and murky environments such as harbors. Advancements in laser imaging systems make highly accurate measurements at further ranges than has previously been possible through temporally filtering of a modulated laser signal at frequencies as high as 1 [GHz]. Here we overview the processes affecting underwater light propagation and visibility, laser imaging systems, recent advancements in the field of underwater optical imaging, and the application of such systems.

ARTICLE INFO

PolHypRes 2021 Vol. 77 Issue 4 pp. 39 – 52

ISSN: 1734-7009 **eISSN:** 2084-0535

DOI: 10.2478/phr-2021-0020

Pages: 14, figures: 5, tables: 0

page www of the periodical: www.phr.net.pl

Publisher
Polish Hyperbaric Medicine and Technology Society

Original article

Submission date: 16.09.2021 r.
Acceptance for print: 27.09.2021 r.

INTRODUCTION - UNDERWATER VISIBILITY

Visibility in the marine environment presents a great challenge, especially when manned underwater diving operations are considered [1] Underwater visibility, z [m] defined in Zaneveld and Pegau [2] was found to be inversely correlated with the attenuation of light as it passes through the water and given as: z 4:8=c, where c [m^{-1}] is the attenuation coefficient [1]. In pure and still water visibility can be sharp over long distances. However, the ocean consists of water filled with chemical compounds, particulate, and micro-organisms that contribute to the attenuation of light that causes visibility to drop sharply from that of pure water; from over 1000 [m] in pure water to around 10-50 [m] in the clear ocean to less than 1 [m] in murky water such as harbors [3].

Underwater imaging systems can be used to drastically increase the range at which objects can be accurately identified when visibility is low [4]. The need to enhance underwater visibility arises in many practical applications such as:

- Diving operations that can be aided by highly accurate imaging of the work-site before divers are submerged.
- High-quality measurements of in-situ debris after hurricanes can help access damage and water navigability.
- Oceanic oil platforms can benefit from highly accurate measurements of the drilling location and equipment to ensure smooth operations.
- The military benefits in areas such as mine warfare and Special Operations [1].

However, various phenomena impede light as it moves through the water. These phenomena have the effects of distorting, blurring, reducing contrast, limiting the distance the light can travel before being extinguished (i.e. absorbed), etc.

Several techniques have been developed for improving underwater optical imaging in scattering media and they are roughly grouped into three basic areas: spatial/temporal filtering, polarization-sensitive detection, and time gating [5].

In this paper, we have focused our attention on the first method, where the backscatter reduction technique is archived by frequency filtering of an optical pulse modulated at microwave frequencies an underwater detection scheme provides orders of magnitude improvement over the presently-existing underwater laser or lidar imaging system. Here we present an overview of the modulated laser imagining systems in underwater applications.

PROCESSES AFFECTING UNDERWATER LIGHT PROPAGATION AND VISIBILITY

Any active optical imaging system consists of a light transmitter, a target, and an optical receiver. The transmitter illuminates the target and the light collected by the receiver carries information about the target. The range at which light can travel before being extinguished, and thus the range of aquatic imaging system, is directly determined by the amount of light scattering and absorption [6]. Typically before the range at which an object is no longer visible is reached, the contrast and resolution, are degraded [7].

In general, absorption decreases the amount of light received, the reflection of the laser of the target yields a weak return (relative to laser power), ambient light reduces contrast, while scattering has the effect of decreasing the contrast caused by the backscattering component and a blurring effect caused by the forwarding scattering component.

More quantitative insight into the effects of absorption and scattering can be gained from analyzing the Radiative Transfer (RT) theory describing time-independent light beam propagation.

MATHEMATICAL DESCRIPTION OF UNDERWATER LIGHT PROPAGATION-RT THEORY

The RT theory can be conveniently expressed in a polar coordinate system where the unit vector $\hat{\xi}$ points in the direction of the laser with $(\theta, \phi) \in \Xi$, where Ξ is the set of all polar angles. The light beam propagates over the solid angle in the direction of the unit vector $\Delta\Omega(\hat{\xi})$. A set of equations derived from Maxwell's equations when expressed in terms of the Poynting vector leads to the Radiative

Transfer Equation [8] given as:

$$\cos\theta \frac{dL(z,\hat{\xi},\lambda)}{dz} = -c(z,\lambda)L(z,\hat{\xi},\lambda) + \int_{\Xi} L(z,\hat{\xi},\lambda)\beta(z,t,\hat{\xi}' \to \hat{\xi},\lambda)d\Omega(\hat{\xi}') + S(z,\hat{\xi},\lambda) \quad [\mathrm{Wm^{-3}sr^{-1}nm^{-1}}] \quad (1)$$

Eq. 1 represents the standard form of the Radiative Transfer Equation (RTE) for unpolarized monochromatic radiance governing the spatial behavior of radiance L = $L(\vec{x},\hat{\xi},\lambda)$ [W m^{-3} st^{-1} nm^{-1}] written in terms of depth (z) [9]. The RTE essential features are discussed below. The component S [W m^{-3} st^{-1} nm^{-1}]is the source function that is the source of light e.g. a laser.

The expression - cL (Eq. 1) is the loss due to attenuation over pathlength L. Lastly, the middle expression $\int_{\Xi} L\beta d\Omega$ gives the contribution of volumetric backscattering (Fig. 1).

A basic property that affects the radiant light field, L, is the total attenuation coefficient [9]:

$$c(z,\lambda) = a(z,\lambda) + b(z,\lambda) \quad (2)$$

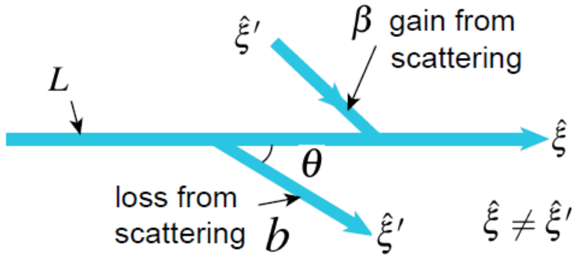

Fig. 1 Illustration of the changes in the radiant light field *L*. Scattering *b* attenuates *L* by scattering light from $\hat{\xi}$ to $\hat{\xi}'$ while also adding to the signal through volumetric scattering $\beta(z,t,\hat{\xi}' \to \hat{\xi},\lambda)$ as light is scattering from $\hat{\xi}$ to $\hat{\xi}'$.

which consist of the absorption *a* and elastic scattering *b*. The distance light will prorogate on average before experiencing scatter, called the mean path-length, is given by the inverse of the attenuation coefficient:

$$\ell \equiv \frac{1}{c} \qquad (3)$$

Attenuation decreases the total signal exponentially as it passes through a non-scattering homogenous medium and represents the simplest solution to the RTE (Eq. 1):

$$I = I_0 e^{-cz}[\mathrm{Wm^{-1}sr^{-1}}] \qquad (4)$$

However, for a complete description absorption and scattering must be accounted for independently.

Typically the absorption is spatially varying and is dependent upon the properties of the medium light moving through [10]. The probability that a particle is not absorbed is equal to 1/*e* (63% of particles absorbed) defines the attenuation length and is equal to ℓ (Eq. 3).

Volume Scattering Function (or β) depends on angle $\hat{\xi}' \to \hat{\xi}$ and is defined as [9]:

$$\beta(z,\hat{\xi}' \to \hat{\xi},\lambda) \equiv \frac{L_*^E(z,\hat{\xi},\lambda)}{L(z,\hat{\xi}',\lambda)\Delta\Omega(\hat{\xi}')}[\mathrm{m^{-1}sr^{-1}}] \qquad (5)$$

The b given by Eq. 5, defines the distribution of the spectra scattering in a volume that can then be conceptualized as the ratio of elastic scattering (L_*^E) over the incident irradiance $(L\Delta\Omega)$.

If we consider the scattering to be circularly symmetric then scattering depends only on angle θ relative to its direction of travel. The scattering coefficient consists of all the scattering over every direction expressed as the integral:

$$b = 2\pi \int_0^{\pi} \beta(\theta,\lambda)\sin\theta d\theta \qquad (6)$$

The typical oceanic β is presented in Fig 2 with elevated β at either very small or large scattering angles.

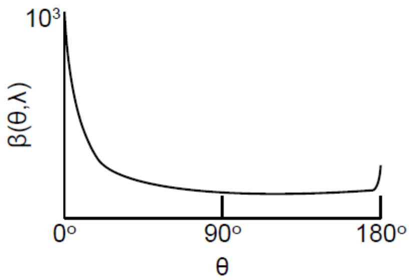

Fig. 2. Sketch of a typical distribution of volumetric scattering $\beta(\theta,\lambda)$ in a scattering medium - Note small scattering angles dominate (forward scattering) and an increase at 180o (back scattering).

To understand the effect of the β angular variability, and noting that the Eq. 1 the L(z) is linear in respect to $\beta d\theta$ we then can separate particle scattering contribution to L(z) as forward, side, and back directions in respect to the original photon path as:

$$b_f = 2\pi \int_0^{10^o} \beta(\theta,\lambda)\sin\theta d\theta \qquad (7)$$

$$b_s = 2\pi \int_{10^o}^{170^o} \beta(\theta,\lambda)\sin\theta d\theta \qquad (8)$$

$$b_b = 2\pi \int_{170^o}^{180^o} \beta(\theta,\lambda)\sin\theta d\theta \qquad (9)$$

From the equations above $b = b_f + b_s + b_b$ (Eq. 6-9) where forward scattering (b_f) is angles from 0^0-10^0, (b_s) is angles from 10^0-170^0, and (b_b) is angles from 170^0-180^0. The choice of limiting a small angle to 10^0 is somewhat arbitrary and is mostly dictated by available observations.

Our conclusions would be relatively insensitive to the choice of that angle and would remain the same if we would have chosen a limiting small angle for example 1^0. The probability of scattering is proportional to $\beta(\theta,\lambda)$ (Eq. 6). Therefore, forward scattering (< 10^0) is typically orders of magnitude more likely when compared to side (90^0) or back (180^0) scattering [11].

That partitioning of scattering effects allows to examine the contributions of scattering from the different types of scattering which have different effects (e.g. the ratio of backscatter to total scattering b_b=b is the ratio of forward scattering to backscattering b_f=b_b). Moreover, we can also examine the mean free path light will travel before experiencing forward, side, or backscattering (e.g. $\ell_f = 1/b_f$). For an understanding of the propagation of light, we need to characterize the light direction and its intensity at every location. This radiant light field can vary over space, time, and wavelength in the ocean dependent upon the contents of the ocean which vary widely (from salt content to micro-organisms). These particulates contribute to the absorption, refraction, reflection, scattered, and depolarization (and more) of the light that interacts with them.

If we don't consider polarization or consider the polarization to be random then absorption (Eq. 4), scattering (Eq. 6), and the volumetric scattering (Eq. 5) are a complete description of the inherent optical properties of a homogeneous medium [3].

Limiting our understanding is the fact that there is a very few closed-form RTE solutions. This leads many researchers to seek numerical solutions [12] or experimental measurements [4] to characterize the nature of the light transfer through the marine environment.

Effect of Absorption and Scattering Underwater on the Target Image

Effects of Absorption

The absorption of the light photons by the water molecules and particles in the water contributes to a decrease in the total signal level collected at the receiver [6]. The effect of absorption, up to point, can be mitigated by selecting the wavelength of the laser light to be in the blue-green region and/or increasing laser power. The absorbed photons are irreversible lost and thus do not contribute to the received signal. However, the propagation of light through the ocean is limited by physical processes beyond absorption.

Effects of Back Scattering

Particle backscattering [6] occurs when transmitted light is reflected off a particulate floating in water: micro-organisms, pollutants, dissolved matter.

In most cases, the backscattered energy reaches the detector without reaching the object. Thus, backscattered by particle light contains no information regarding the object and it reduces the image contrast and resolution as well as the object ranging measurement accuracy.

Effects of Forward Scattering

Forward scattering occurs due to the light interacting with water-suspended particulate and background turbulence.

Forward scatter light contains scrambled information about the distance and location of the target due to its longer path length and deflection. The effects of forward scattering on a single photon path are illustrated in Fig 3.

Here the photon light trajectory due to forward scattering is changed by a small angle, typically (« 10^0), with respect to its original trajectory before the forward scattering event.

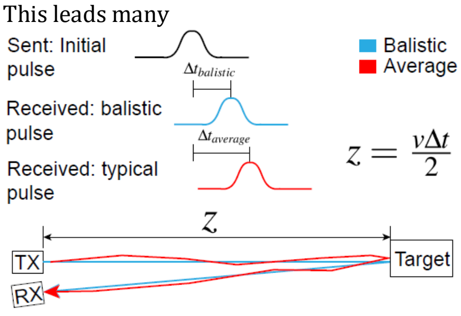

Fig. 3 A modulated pulse of laser light emitted and received by a transmitter (TX) and receiver (RX) has a phase difference equivalent to the time difference (Δt) (shown in blue) whereby the distance to the target (z) can be calculated given the velocity of light through the medium (v). However, if multiple scattering occurs the time difference will result in a longer return time (shown in red).

In the oceanic environment, the near-forward part of the oceanic volume scattering function, β, is driven by an interaction of light with turbulent inhomogeneities of the water refractive index Bogucki et al. [13], arising mostly as the effect of water temperature fluctuations.

These turbulent-induced inhomogeneities are very effective light scatterers at near-forward angles. It has been documented in aquatic VSF measurements of Bogucki et al. [14] that in the range of $\theta_1 = 10^{-7}$ to $\theta_2 = 10^{-3}$ rad, the scattering coefficient b_{turb} exclusively due to turbulent inhomogeneities (defined as: $b_{turb} = 2\pi \int_{\theta_1}^{\theta_2} VSF(\theta) sin(\theta) d\theta$) can easily attain value of b_{turb} = 10m-1. Such large value of the b_{turb}, implies that the photon mean pathlength between scattering events ℓ_{turb} on turbulent inhomogeneities is around few centimeters, since $\ell_{turb} \approx 1/b_{turb}$. That path length is much shorter than the typical mean path length due to scattering by particles which is around a few meters to tens of meters Mobley [8]. Consequently, most of the lidar or laser line scanner detected photons undergo many multiple forward scattering on turbulence events and a single backscattering event on a target or water-suspended particle.

Using this knowledge of light interaction with the aquatic environment, it is possible to design systems that can overcome signal reduction by elastic scattering events.

How these physical limitations are overcome by modern underwater image systems and how these systems work are described in the sections below.

LASER IMAGE SYSTEMS (LIS) IN AQUATIC APPLICATIONS

Typically image systems use moveable mirrors to steer the laser beam. The steering of the beam can be onedimensional (with the motion of the system contributing to the other dimension) as inside a laser printer, or just two-dimensional. The synchronously received information from a LIS system is typically stored as an image of the target. The minimum water absorption happens at wavelengths of light around 418 [nm] with an absorption coefficient of 0:0044 [m-1] [10]. Therefore, the light used to capture underwater images tend toward the blue-green area of the spectrum near the minimum.

The image formed after the light is emitted and captured consists of the direct light that was reflected off the target (light containing correct distance and location metric scattering function (Eq. 5) that's had no interaction with the target (reduces contrast), and a forward scattering component of the volumetric scattering (blurs image).

Deployment of LIS (particularly in the deep ocean) requires a stable platform. Navy submarines make a very ideal choice for this technology due to their stability, power supply, and nearly unlimited depth, such as MacDonald et al. [15] who mounted an LSS on the US Navy Submarine NR-1. On this ideal platform, the LIS was able to collect 40 [m] swaths which can be mosaicked into a 1 [km2] image. NR-1 during her 11-day mission was able to collect centimeter-level accurate images of [15]; two drilling templates located at 450 and 650 [m] depths, chemosynthetic tube worms located at natural oil seeps, a brine pool surrounded by methanotrophic mussels, an active mud volcano, and 50 [km] of a pipeline.

Advances in computing and battery power made it possible for LIS to be deployable on common-sized AUV [16] rather than a nuclear submarine.

The benefits of the accessibility of this technology to all ocean sciences, ocean oil and gas exploration, and the military could be substantial. Detailed millimeter-level accurate maps of ocean topography can be collected for use by all parties, such as the ocean floor slope and surface roughness [17]. Mapping of oil pipelines, as noted by [15], could be used to determine where currents are running under the pipeline as well as maps of the floor for use in drilling operations.

Other applications include those relating to diving operations, particularly where precise tools and repairs are concerned, where accurate measurements and the condition of the work site can be critical such as; the extent of damage, potential hazards, and the size of fittings.

LASER LINE SCANNERS (LLS)

To mitigate the effects of scattering both a narrow source (e.g. laser) and receiver (e.g. captures the light coming from a narrow direction) both decrease the amount of scattered light emitted and received [3]. This realization has led to the development of Laser line scanners (LLS) for use in underwater imaging. LLS uses a Continuous Wave (CW) laser that systematically and synchronously scans a target area. The reflected light from the target is detected by a light sensor. To overcome the limitations of attenuation (Eq. 4) LLS systems used underwater need a powerful laser to achieve a sufficient return.

LIDAR METHODS

By use of the lidar methods, it is possible to gather distance information about the imaging target. The method works by modulating a pulsed laser within the microwave band and extracting the modulations after being received.

The extracted modulation from the returned light can be measured against the phase of the initial pulse whereby the temporal offset can be determined and distance calculated, (Fig. 3). However, if multiple scattering occurs the time difference will result in an error in distance measurements (Fig. 3).

A lidar type system can be of great use in scattering environments since they gate out the near-field backscatter by synchronizing the pulse of the light source with the opening and closing of a gate to the detection element [5]. However, the gating needs to be very quick since the effects of scattering are significant.

Given that light travels 22.5 cm/ns in the ocean, nanosecond pulses are needed to have a range of accuracy of 10 s of centimeters in the cloudiest water [3]. An example developed by Churnside et al. [18] used a laser at 532 [nm] with 600 [mJ] of power and a variable range gate that could image light from 3 [ns] to 100 [ps] during emission.

Using this method it is possible to eliminate most of the backscattering which improves the image quality and range of the device.

The underwater configure consist of a high-powered narrow blue-green laser and narrow receiver that is capable of opening a gate on the order of picoseconds after the pulse is emitted. However, if the operation of the underwater

LIS is in coastal waters where the attenuation tends towards scattering dominant then the resultant imaging will be of poor quality due to excessive blurring and a reduction in contrast which decrease. Turbid water, with a large concentration of particulate, and with a relatively smaller turbulent flow contribution to forward scattering, can lead to distortion and blurring of the images [19].

IMPROVED LIS DETECTION RANGE - SPATIAL/TEMPORAL FILTERING

The promising method to improve LIS detection range, the hybrid lidar-radar, works by filtering out light arriving at the RX in that way that we can split the received signal into light directly reflected off the target (ballistic component) and typical or reflected off the target but also scrambled by the forward scattering, Fig 3. The hybrid lidar-radar approach permits the rejection of noise contained associated with multiple forward scattering events.

The use of a hybrid lidar-radar approach was first done by Mullen and Contarino [20] that combined the detection and signal-processing techniques of radar with the optical characteristics of lidar. The technique used a modulated signal combined with a radar (optical) receiver to measure the difference in the modulation of the light to properly reject the light that is not minimally scattered. If the water is turbit or murky forward scattering becomes the primary issue which much is corrected as noted above. To achieve this a laser is modulated temporally at microwave frequencies.

The primary method to gain improvements in underwater images relies on a temporally modulated laser pulse.

Mullen et al. [21] showed by temporally modulating the waveform LIS was able to filter out some of the solar and near-field backscattering. The method employed a modulated laser at microwave frequencies from 10 [MHz] to 90 [MHz] where backscattering and multiple forward scattered light will be demodulated with respect to the directly reflected light. Cochenour et al. [22] shown experimentally that the angular distribution of forward scattering decreased as the modulation frequency increased - as high as 1 [GHz]. The decrease in forward-scattering enhances the spatial resolution [7] modulated (1GHz) light had a decrease in the amount of light that was multiply scattered due to destructive interference. This is illustrated in figure 4 where the higher modulation frequency (1 [GHz]) deconstructively interferes with multiply scattered light while the lower modulation frequency (500 [MHz]) maintains its modulation frequency and the interference is constructive for the same path-length difference. Therefore, the higher frequency light that arrives at the sensor which is still modulated comprises more light that has lower order scattering compared to lower modulation frequency [23]. The trade-off of higher modulation frequency is that the modulation amplitude decreases sharply after 10 attenuation lengths which are negatively affected by the increasing modulation. This is due to higher frequency modulations being more susceptible to scattering [4].

SPATIAL FILTERING & ORBITAL ANGULAR MOMENTUM (OAM)

Through spatial filtering, it is possible to remove backscatter. Perez et al. [24] notes that the phase of the volumetric backscatter is independent of the system's (laser-receiver) movement while the system's phase is dependent on it. They found by encoding multiple modulation frequencies the spatial filtering reduced the absolute signal to noise (compared to unfiltered) of an object measured at close range. It was found by Cochenour et al. [23] that by measuring the orbital angular momentum in a turbit underwater channel it was possible to spatially discriminate between the return signal and backscattered light around 2 attenuation lengths. An optical vortex, created by passing the light through a diffractive spiral phase plate, was used to enhance the range detection accuracy of the laser ranging system by Jantzi et al. [25] by being able to discriminate the spatial relationship between coherent and incoherent light.

APPLICATIONS OF THE LIS WITH TEMPORAL FILTERING FOR UNDERWATER TARGET DETECTION AND/OR OAM

Temporal filtering enables LIS to be able to see in a greater variety of underwater locations due to the filtering significantly increasing the range and accuracy of imaging.

Specifically, the method enables LIS to be used in murky and turbid environments due to the ability to filter out forward scattered light. However, the practical application of a high-frequency modulated LIS requires modification to the design of the modulated waveform.

Distinguishing time differences between modulating light requires a large bandwidth (bigger than the bandwidth needed to distinguish forward scattered light). This can be overcome by having a Gaussian pulse train and making measurements in the frequency domain where several measurements can be made by centering a narrow bandwidth receiver around each frequency harmonics. As seen in figure 5 a Gaussian pulse train modulated at 1 [GHz] will produce a frequency response peaking at the modulation frequency and every integer multiple of it out to the Nyquist frequency. Thus, a LIS can make measurements with reduced bandwidth, higher dynamic range, and sensitivity [22]. The high-frequency components can be split into an intermediate frequency where low sample rate and high-resolution digitizers can be used.

Detailed by Cochenour et al. [22]: a wideband spectrum can be generated using a mode-locked laser that outputs a Gaussian pulse train defined by

$$P_{opt}(t) = \frac{\bar{P}_{opt}}{\sqrt{2\pi}} \frac{T}{t} \sum_{n=-\infty}^{\infty} \exp[-(t+nT)^2/2\tau^2] \qquad (10)$$

where $\bar{P}_{opt}$ is the average transmitted optical power, T is the pulse repetition period, and τ is the Gaussian pulse time constant. The Fourier transform of Eq. 10 yields an output as observed by a detector before attenuation of the signal of,

$$P_{ac}(f) = P_{dc} \times \exp[-(2\pi\tau f)^2] \qquad (11)$$

where $P_{ac}(f)$ is the electrical power at frequency *f*, the averaged DC component $P_{dc} = R_L(\mathscr{R}P_{opt})^2$, where R_L is the load resistance and $\mathscr{R}$ is the detector responsivity. After the laser passes through water and is attenuated the signal would be received by the photodetector given by

$$P_{ac}(f, cz) = m(f, cz) \times P_{dc}(cz), \qquad (12)$$

where c [m^{-1}] is the attenuation coefficient (Eq. 4). The term m(*f,cz*) is the modulation depth that represents a fractional $(0 < m(f, cz) \leq 1)$ amount of power loss due to forward scattering. The implication of Eq. 12 is that the power loss occurs due to absorption and scattering is frequency independent and loss occurs due to forward scattering that is frequency dependent. Therefore, through of

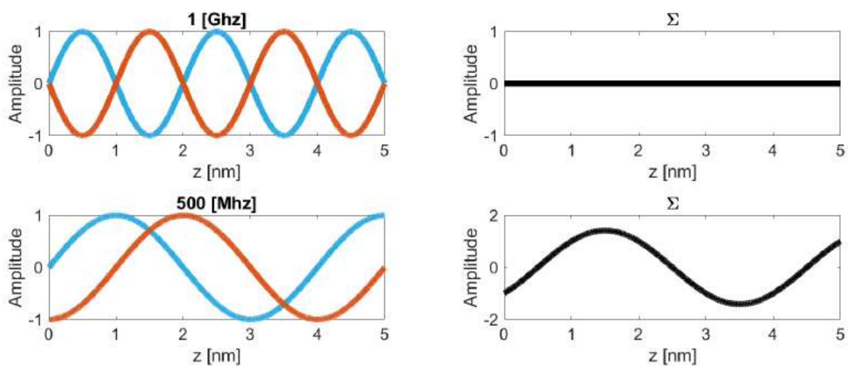

Fig. 4 Illustration of wave interactions due to different modulation frequencies of 1 [Ghz] and 500 [MHz]. The ballistic light (blue) is joined by multiply scattered light (red) where the waves interact.

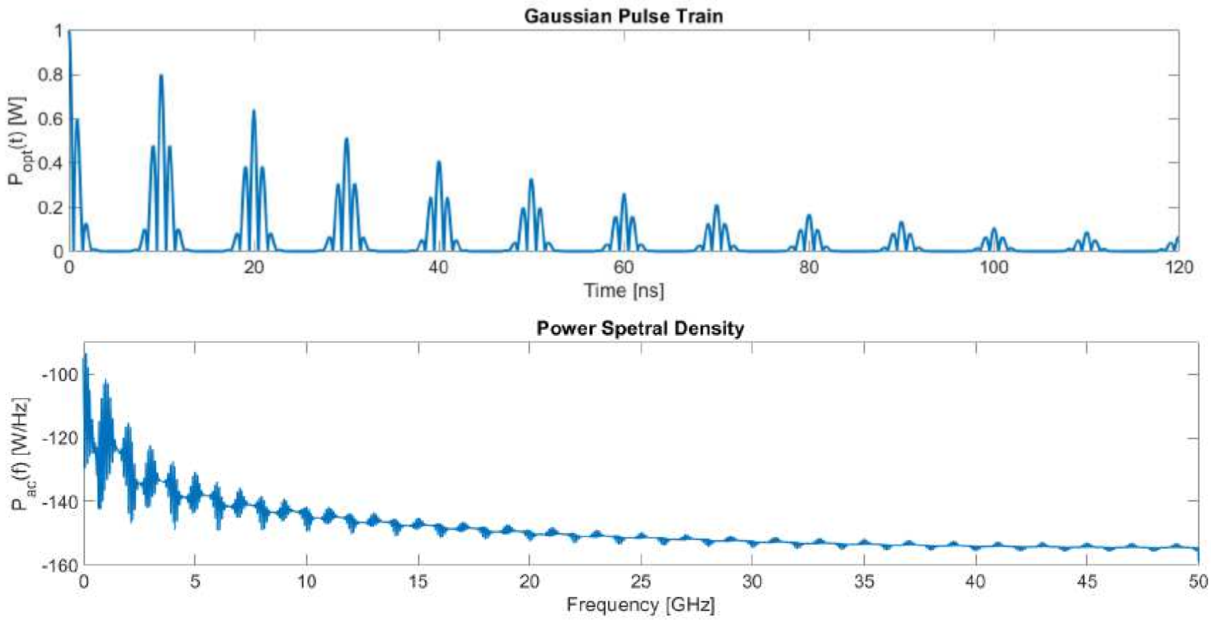

Fig. 5 A Gaussian pulse train modulated at 1 [GHz] $P_{dc}(t)$ with a pulse every 10 [ns] exponentially decaying over 120 [ns] accompanied by the power spectral density $P_{ac}(f)$ [W/MHz].

Eq. 10 & 11 Cochenour et al. [22], a technique borrowed from Gloge et al. [26] and Helkey et al. [27] was able to generate a signal rich in frequency content (Fig. 5) without a wideband receiver at an attenuation length of cz = 0:684 in clear water to cz = 15:88 in turbid water. However, there is a significant decrease in the modulation depth [dB] after ~ 10 attenuation lengths (cz) compared to lower modulation frequencies [4].

However, noted by Cochenour et al. [22], there are several practical issues to overcome when implementing this technique when imaging underwater as state-of-theart equipment was used in a laboratory setting. Yet, it was shown to improve contrast by filtering out forward scattered light.

CONCLUSIONS AND FUTURE WORK

- Underwater visibility is inversely correlated with attenuation of light $z \approx 4.8/c$ [1] (i.e. 4:8 attenuation lengths). Visibility decreases sharply in turbid and/or murky environments.
- Underwater visibility is affected by the attenuation of the light from both scattering and absorption. Attenuation comprised of both scattering and absorption (Eq. 2) which decreases the signal exponentially (Eq. 4). Scattering also has the effect of blurring and distorting the image through the volumetric scattering function (Eq. 5).
- LLS systems enable a laser to systematically scan a target area to produce a 2D image of the target area. While lidar methods, that modulate the laser, enable the distance to the target to be known with a high degree of accuracy.
- Modulation of the laser at microwave frequencies enables temporal filtering of light that is not minimally scattered [21].
- Higher modulation frequencies (up to 1 [GHz]) cause destructive interference of light which decreases the angular distribution of light [4].
- Through the work of Cochenour et al. [22] a modulated LIS system can be designed to be capable of measuring to a high degree of accuracy in turbid or murky environments to _ 10 attenuation lengths (cz) without a significant decrease in modulation depth.
- It is also possible to impart OAM to the signal to increase the detection range.
- Advances in communications technology that modulate waves in the millimeter wave (30–300 [GHz]) that have come due to the roll-out of the 5G infrastructure have driven down the cost of the necessary components which are mass produced. This enables developers of this technology to turn to commercially available products instead of state-of-the-art equipment which drastically drives down the cost of a LIS.
- We intend to design a system that can implement the technique described herein to be deployable in the marine environment.

REFERENCES

1. Zaneveld, J., and W. S. Pegau, 2003a: The prediction of diver visibility and its relation to spectral beam attenuation. Tech. rep., WESTERN ENVIRONMENTAL TECHNOLOGY LAB INC (WET LABS INC) PHILOMATH OR.
2. Zaneveld, J. R. V., andW. S. Pegau, 2003b: Robust underwater visibility parameter. Optics express, 11 (23), 2997–3009.
3. Jaffe, J. S., 2014: Underwater optical imaging: the past, the present, and the prospects. IEEE Journal of Oceanic Engineering, 40 (3), 683–700.
4. Cochenour, B., K. Dunn, A. Laux, and L. Mullen, 2017a: Experimental measurements of the magnitude and phase response of high-frequency modulated light underwater. Applied optics, 56 (14), 4019–4024.
5. Dalgleish, F. R., A. K. Vuorenkoski, and B. Ouyang, 2013: Extendedrange undersea laser imaging: Current research status and a glimpse at future technologies. Marine Technology Society Journal, 47 (5).
6. Stramski, D., E. Boss, D. Bogucki, and K. J. Voss, 2004: The role of seawater constituents in light backscattering in the ocean. Progressin Oceanography, 61 (1), 27–56.
7. Luchinin, A., and L. Dolin, 2014: Application of complex-modulated waves of photon density for instrumental vision in turbid media. Doklady Physics, Pleiades Publishing, Vol. 59, 170–172.
8. Mobley, C. D., 1994a: Light and water: radiative transfer in natural waters. Academic Press.
9. Mobley, C. D., 1994b: Light and Water. Radiative Transfer in Natural Waters. Academic Press.
10. Pope, R. M., and E. S. Fry, 1997: Absorption spectrum (380–700 nm) of pure water. ii. integrating cavity measurements. Applied optics, 36 (33), 8710–8723.
11. Petzold, T. J., 1972: Volume scattering functions for selected ocean waters. Tech. rep., Scripps Institution of Oceanography La Jolla Ca Visibility Lab.
12. Luchinin, A. G., and M. Y. Kirillin, 2016: Temporal and frequency characteristics of a narrow light beam in sea water. Applied Optics, 55 (27), 7756–7762.
13. Bogucki, D., J. A. Domaradzki, D. Stramski, and R. Zaneveld, 1998: Comparison of nearforward scattering on turbulence and particles. Atmos.–Ocean, 37, 4669–4677.
14. Bogucki, D., J. Domaradzki, C. Anderson, H. Wijesekera, R. Zaneveld, and C. Moore, 2007: Optical measurement of rates of dissipation of temperature variance due to oceanic turbulence. 15 (12), 7224–7230.
15. MacDonald, I. R., J. S. Chu, F. Reilly, M. Blincow, and D. Olivier, 1995: Deep-ocean use of the sm2000 laser line scanner on submarine nr-1 demonstrates system potential for industry and basic science. 'Challenges of Our Changing Global Environment'. Conference Proceedings. OCEANS'95 MTS/IEEE, IEEE, Vol. 1, 555–565.
16. Dalgleish, F., F. Caimi, W. Britton, and C. Andren, 2007: An auvdeployable pulsed laser line scan (plls) imaging sensor. OCEANS 2007, IEEE, 1–5.
17. Wang, C.-C., and D. Tang, 2009: Seafloor roughness measured by a laser line scanner and a conductivity probe. IEEE Journal of Oceanic Engineering, 34 (4), 459–465.
18. Churnside, J. H., J. J. Wilson, and V. V. Tatarskii, 2001: Airborne lidar for fisheries applications. Optical Engineering, 40 (3), 406 – 414, doi:10.1117/1.1348000, URL https://doi.org/10.1117/1.1348000.
19. Hou, W., S. Woods, E. Jarosz, W. Goode, and A. Weidemann, 2012: Optical turbulence on underwater image degradation in natural environments. Applied optics, 51 (14), 2678–2686.
20. Mullen, L. J., and V. M. Contarino, 2000: Hybrid lidar-radar: seeing through the scatter. IEEE Microwave magazine, 1 (3), 42–48.
21. Mullen, L. J., V. M. Contarino, A. Laux, B. M. Concannon, J. P. Davis, M. P. Strand, and B. W. Coles, 1999: Modulated laser line scanner for enhanced underwater imaging. Airborne and In-Water Underwater Imaging, SPIE, Vol. 3761, 2–9.
22. Cochenour, B., S. P. O'Connor, and L. J. Mullen, 2013: Suppression of forward-scattered light using high-frequency intensity modulation. Optical Engineering, 53 (5), 051 406.

23. Cochenour, B., L. Rodgers, A. Laux, L. Mullen, K. Morgan, J. K. Miller, and E. G. Johnson, 2017b: The detection of objects in a turbid underwater medium using orbital angular momentum (oam). Ocean Sensing and Monitoring IX, SPIE, Vol. 10186, 1018603.
24. Perez, P., W. D. Jemison, L. Mullen, and A. Laux, 2012: Techniques to enhance the performance of hybrid lidar-radar ranging systems. 2012 Oceans, IEEE, 1–6.
25. Jantzi, A., W. Jemison, A. Laux, L. Mullen, and B. Cochenour, 2018: Enhanced underwater ranging using an optical vortex. Optics express, 26 (3), 2668–2674.
26. Gloge, D., E. Chinnock, and D. Ring, 1972: Direct measurement of the (baseband) frequency response of multimode fibers. Applied Optics, 11 (7), 1534–1538.
27. Helkey, R., D. Derickson, A. Mar, J.Wasserbauer, and J. Bowers, 1993: Millimeter-wave signal generation using semiconductor diode lasers. Microwave and optical technology letters, 6 (1), 1–5.